Supporting Information

Durable of Cu_xO/Mesoporous TiO_2 Photocatalyst for Stable and Efficient Hydrogen Evolution

Lingling Cui,[a,†] Chunyao Niu,[b,†] Young Soo Kang,[c] Rachel A. Caruso[d] and Xiao Li Zhang[a,]*

[a]School of Materials Science and Engineering, Zhengzhou University, 450001 P.R. China.

[b]School of Physics and Microelectronics, Zhengzhou University, 450001 P.R. China.

[c]Environmental and Climate Technology, Korea Institute of Energy Technology (KENTECH), 200 Hyeoksin-ro, Naju City, Jeollanamdo 58330, Korea.

[d]Applied Chemistry and Environmental Science, School of Science, RMIT University, Melbourne, VIC 3001, Australia.

†Equal contribution.

*Corresponding author. E-mail: xiaolizhang.z@gmail.com.

Experimental Details

Chemicals

Chemicals used in the material syntheses were all reagent grade from Sinopharm Chemical Reagent Co., Ltd (Shanghai, China) including acetonitrile, butan-1-ol, titanium butoxide (97%), ammonia (28%), ethanol, sodium hydroxide, hydrochloric acid (37%), copper acetate (98%) and methanol. Degussa P25 TiO_2 nanoparticles from Evonik were used in the control experiments. Milli-Q water (18.2 mΩ/cm) was used throughout.

Materials synthesis

To form an amorphous titania the following approach was used.[1] Titanium butoxide (7.16 mL) was added drop-by-drop to a solvent mixture of acetonitrile and butan-1-ol (volume ratio of 1:1, 200 mL) under moderate stirring. The stirring continued until a clear solution was obtained, approximately 20 mins. A second solution containing the same solvent mixture, as well as 3.6 mL of distilled water and 2.7 mL of ammonia was quickly added to the titanium butoxide solution under moderate stirring and a white precipitate formed within a few seconds. The solution was stirred for 2 h then the white precipitate was collected by centrifugation and washed with ethanol 3 times before being redispersed in 30 mL of 5 M sodium hydroxide solution. The solution was transferred into a Teflon-lined stainless-steel autoclave (50 mL in capacity) for solvothermal reaction at 140 °C for 10 h. The products were washed with water and collected by centrifugation 3 times to remove residual sodium hydroxide. The sodium titanate (0.02 mol) was redispersed in 500 mL of a hydrochloric acid solution of various concentration (0.05, 0.10, 0.15, 0.20 and 0.25 M). The precipitates collected by centrifugation

were redispersed in highly concentrated aqueous copper acetate solution (0.30 M) under magnetic stirring for 20 min to remove the remaining sodium. After washing with water and ethanol several times and drying at room temperature overnight, copper titanates with varying copper loadings were obtained. The samples were calcined at 450 °C for 1 h in air with a temperature ramp rate of 2 °C/min using a muffle furnance, decompositing the copper titanate and oxidising the copper. The samples were labelled as CT1, CT2, CT3, CT4, and CT5, corresponding to the increasing HCl concentrations. CT3-500 sample referes to the CT3 prepared using a calcination at 500 °C for 1 h in air.

A porous TiO_2 control sample was prepared as follows. Sodium titanate was protonated by 500 mL 0.50 M hydrochloric acid solution. The obtained hydrogen titanate was washed with water and ethanol several times before drying at room temperature overnight and calcining at 450 °C for 1 h in air. The sample was labelled as T.

Cu_xO/TiO_2 composite control samples based on Degussa P25 TiO_2 nanoparticles were prepared through wet-impregnation to obtain the same copper loading as CT1-CT5 (based on the ICP-OES analysis results). P25 TiO_2 nanoparticles (1.00 g) was dispersed in a copper acetate aqueous solutions of various concentrations to form a suspension which was slowly dried at 60 °C under moderate magnetic stirring. The obtained powder was calcined at 450 °C for 1 h in air to oxidise the copper. The samples were labelled as P1, P2, P3, P4, and P5, corresponding to the copper loading in CT1, CT2, CT3, CT4, and CT5, respectively.

Characterization

A JEM-2100F, JEOL transmission electron microscope (TEM) was used to investigate the morphology and conduct elemental mapping of the samples. X-ray diffraction (XRD) patterns obtained on an X-ray diffractometer (UItima IV) using Cu Kα irradiation under a 40 kV working voltage were used to determine the crystal phases of the obtained samples. Raman spectra were acquired on a HORIBA Lab-RAM HR-Evolution Raman spectrometer with laser excitation at 532 nm. The UV/Vis diffuse reflectance spectra (UV/Vis DRS) were obtained with a UV/Vis/NIR spectrophotometer (UH4150, Hitachi, Japan) in the wavelength range 300-800 nm. The photoluminescence spectra were recorded on a fluorenscence spectro-photometer (F-280-Laser-NIR, Gangdong Science and Technology Development Co., LTD. Tianjin) with an excitation wavelength of 460 nm. X-ray photoemission spectra were collected using a Thermo Escalab 250xi analyzer. Cu 2p and Ti 2p binding energies were recorded using Al Kα (1486.6 eV) as the excitation source and a pass energy of 23.5 eV. The position of the XPS peaks of the corresponding element is referenced to the C1s peak of carbonaceous contamination. A Micromeritics Tristar 3000 system was used to measure the nitrogen sorption isotherms of the samples after being degassed at 100 °C on a vacuum line overnight. Specific surface area and pore size were evaluated by using a standard Brunauer-Emmett-Teller (BET) analysis. Adsorption curves were used to provide pore size distributions.

Inductively Coupled Plasma - Optical Emission Spectroscopy (ICP-OES, Perkin Elmer OPTIMA 7300) was used to analyse the copper loading in the mesoporous Cu_xO/TiO_2 composites (CT1-CT5). 100 mg of sample was digested in 3 mL of sulfuric acid (98%) by heating at 80 °C for 30 min. The obtained solution was diluted with 20 mL distilled water and filtered

before being transferred into a 100 mL volumetric flask and diluted to 100 mL with distilled water. The copper content in the solution was analysed by the ICP-OES.

Photocatalytic hydrogen generation

The photocatalytic hydrogen evolution experiments were carried out at room temperature (20 ± 1 °C) controlled by a cooling system and in a vacuum sealed reaction system. The powdered photocatalyst (10 mg) was ultrasonically dispersed in a 50 mL methanol aqueous solution (volume ratio of 1:4) in a Pyrex flask (350 mL) with a flat window that was illuminated with a 300 W Xe lamp (Perfect Light, PLS-SXE300D). Gas evolution was determined by an online gas chromatograph (GC-7860, Ar carrier gas).

Computational simulation details

The first-principle calculations were performed within the density functional theory (DFT) plane-wave pseudopotential method, as implemented in the Vienna Ab-initio Simulation Package (VASP code).[2, 3] The exchange-correlation energy and the core electrons were considered using the generalized gradient approximation by the Perdew-Burke-Ernzerhof functional[4] and the projector augmented wave pseudopotentials,[5] respectively. For the Ti 3d orbitals, Cu 3d orbitals, O 2p orbitals of TiO_2, and O 2p orbitals of Cu_2O and CuO, the Hubbard U correction was carried out and the corresponding U values were set to 3.5, 6.8, 3.5, and 12 eV, respectively.[6, 7] A plane-wave cutoff energy of 450 eV was used. All atoms were fully relaxed with a tolerance in total energy of 10^{-5} eV, and the forces on each atom were less than 0.02 eV/Å. The zero-damping DFT-D3 method[8] of Grimme was amended to correct for the vdW interaction in the DFT-vdW calculations. To model the TiO_2 surface, the dominant (101) facet

was used, while for the Cu_2O and CuO surfaces, the most stable (111) surfaces were used. The Cu_{10} cluster was used to model the surface with Cu atoms.The experimental bulk lattice parameters of TiO_2, Cu_2O, and CuO were used for the surface calculations throughout the present work. A vacuum of 16 Å perpendicular to the surface was applied to avoid the interaction between adjacent periodic slabs.

The adsorption energy of hydrogen atom (E_{ad}) is defined as the energy difference after and before the adsorption with respect to the gas phase H_2 molecule according to $E_{ad}=E_{total}-E_{surface}-1/2E_{H2}$, where $E_{surface}$, E_{H2}, and E_{total} are the energies for the clean surface, H_2 molecule in the gas phase, and hydrogen atom adsorbed on the surface, respectively. The hydrogen absorption free energyΔG_H is obtained by adopting the entropy correction proposed by Norskov *et al.* according to $\Delta G_H=E_{ad}+0.24$ eV.[9]

Table S1. The copper loading in the mesoporous Cu_xO/TiO_2 composites (CT1-CT5) based on the ICP-OES analyses.

Sample	Cu (wt%)
CT1	8.6
CT2	7.7
CT3	6.8
CT4	4.7
CT5	3.9

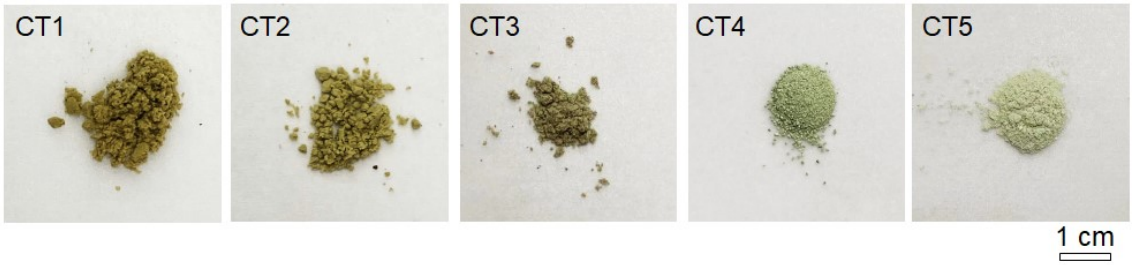

Figure S1. Optical images of the mesoporous Cu_xO/TiO_2 composites.

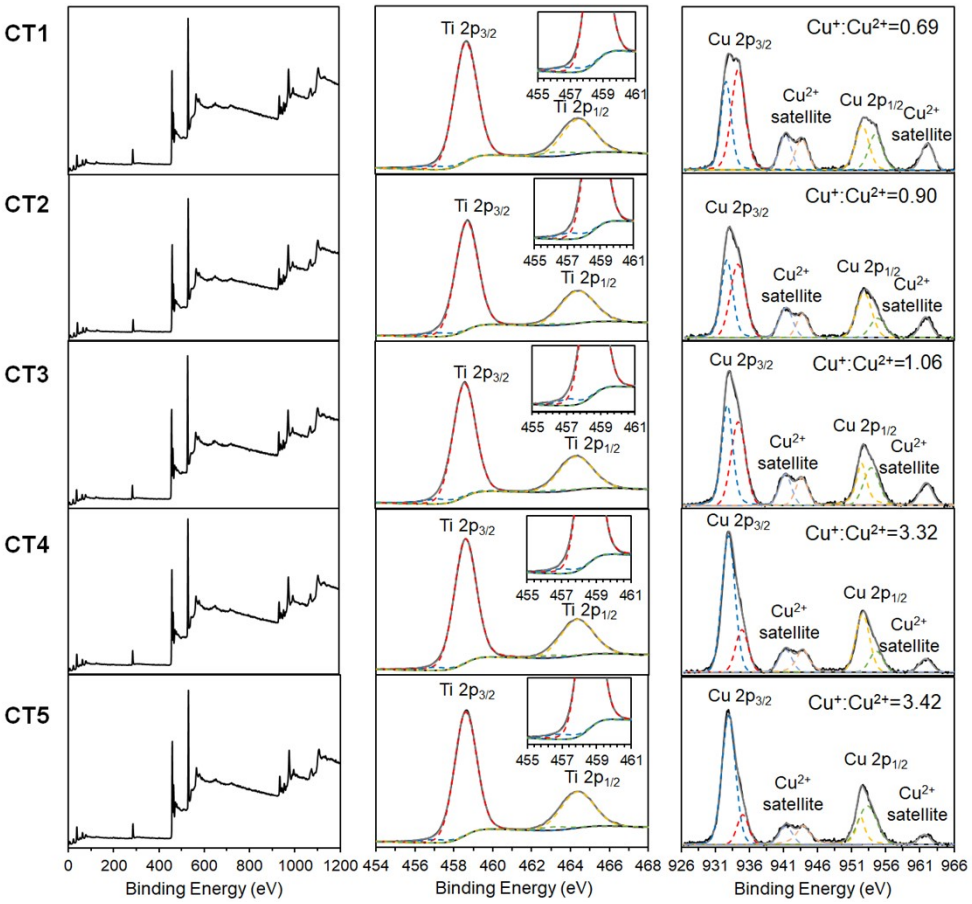

Figure S2. XPS spectra (left) and peak fitting of Ti 2p (middle) and Cu 2p (right) of the mesoporous Cu_xO/TiO_2 composites: CT1, CT2, CT3, CT4, and CT5.

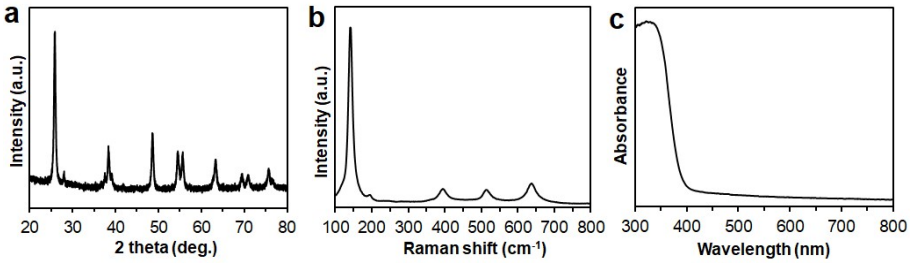

Figure S3. a) XRD pattern, b) Raman spectra and c) UV-vis absorbance spectra of the mesoporous TiO_2, sample T.

Table S2. Hydrogen evolution rate and reaction conditions of Cu-based TiO_2 composites from literature compared to sample from this work.

Photocatalyst	Scavenger	Light source	HER (mmol/g/h)	Reference
Cu_xO/TiO_2	20% methanol	300 W Xe lamp	12.45	This work
Cu_2O/TiO_2	10% methanol	150 W Xe lamp	~0.30	10
CuO QDs/TiO_2	10% methanol	300 W Xe lamp	2.00	11
Cu_2O/TiO_2 shell/core nanorods	20% methanol	300 W Xe lamp	1.52	12
Cu_2O/TiO_2	20% methanol	300 W Xe lamp	7.14	13
Cu/Cu_2O/(001)-TiO_2	20% methanol	300 W Xe lamp	18.39	14
Cu/CuO/TiO_2	25% methanol	300 W Xe lamp	8.51	15
Single-atom Cu/TiO_2	25% methanol	300 W Xe lamp	16.6	16
CuO/P25-TiO_2	20% methanol	500 W Xe lamp	8.23	17
CuO nanodots/TiO_2	10% methanol	100 W Hg lamp	~16.50	18
CuO/TiO_2	50% methanol	1 Solar light	4.76	19
Cu_2O/(001) faceted TiO_2 Cu_2O/(101) faceted TiO_2	10 % methanol	300 W Xe lamp	~0.84, 1 wt% Pt 32.60, 1 wt% Pt	20
Hollow Cu-TiO_2/C nanospheres	10 % methanol	300 W Xe lamp	14.05, 0.2 wt% Pt	21

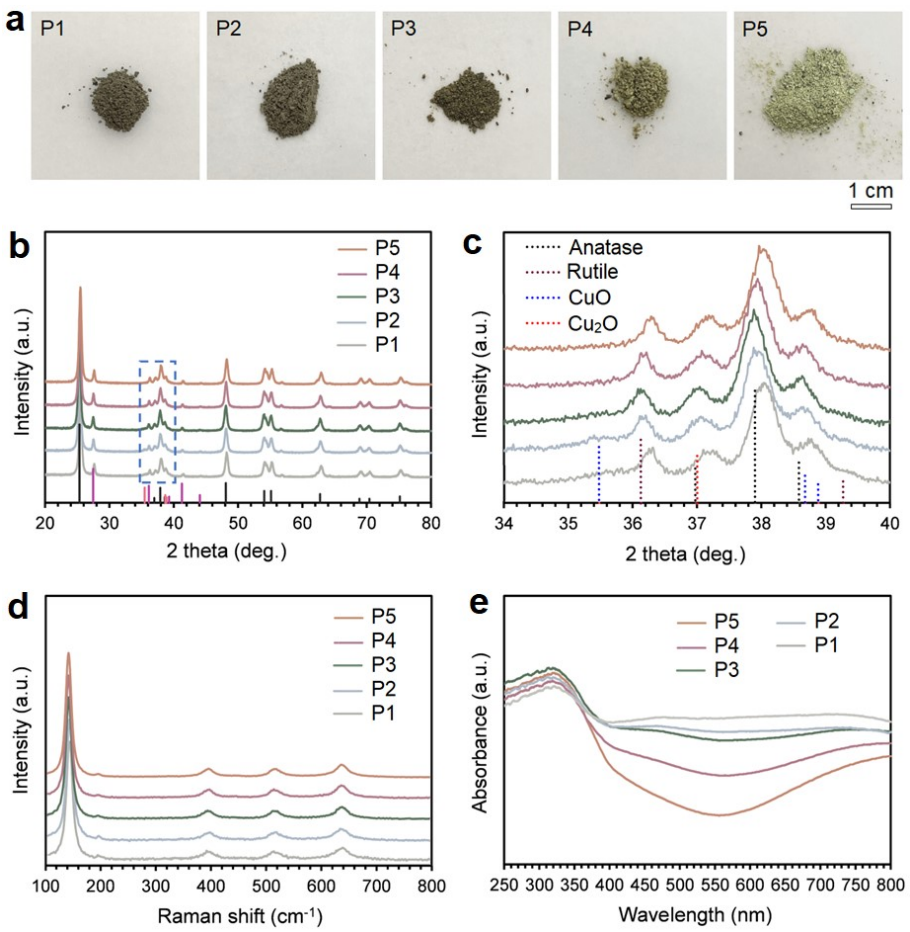

Figure S4. a) Optical images, b) XRD patterns, c) enlargement of the XRD patterns from 34-40° 2θ, d) Raman spectra and e) UV-vis absorbance spectra of the P25-based Cu_xO/TiO_2 composites control samples (P1, P2, P3, P4, and P5) with the same copper loading as that of the mesoporous Cu_xO/TiO_2 composites.

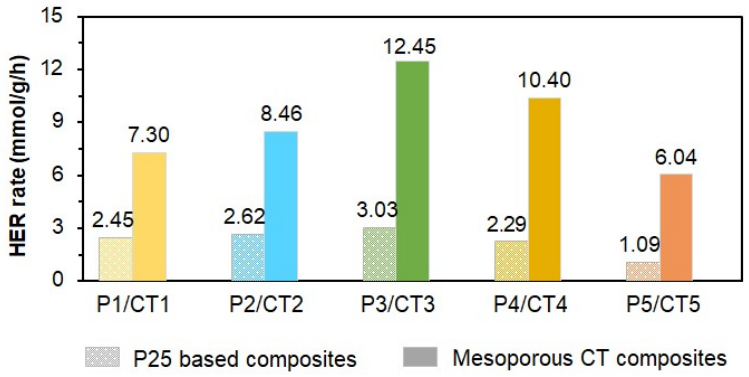

Figure S5. HER rate for the mesoporous Cu_xO/TiO_2 composites and the P25-based Cu_xO/TiO_2 composites with the same copper loading.

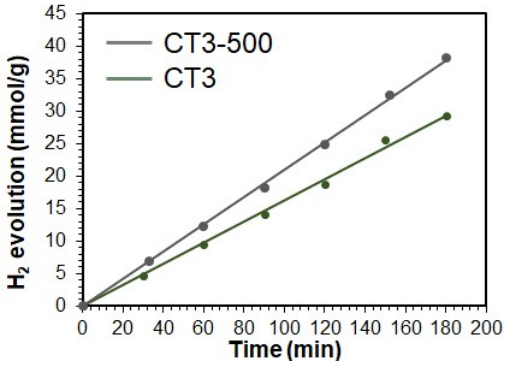

Figure S6. H_2 evolution for CT3 and CT3-500.

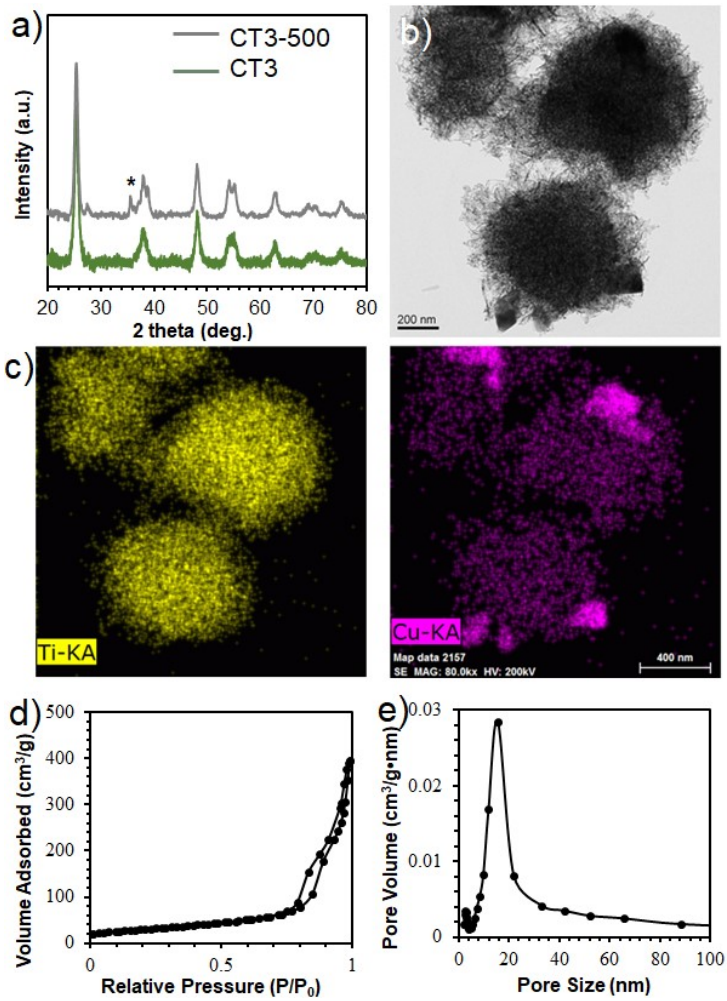

Figure S7. (a) XRD patterns of CT3 and CT3-500 (* indicates the characteristic peak of CuO). (b) TEM image, c) elemental mapping analyses for Ti (left) and Cu (right), d) nitrogen sorption isotherm and e) pore-size distribution curves of CT3-500.

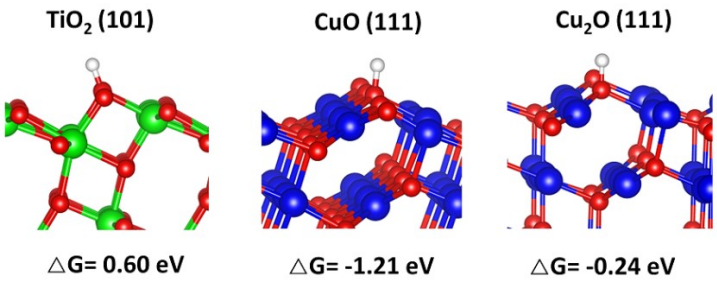

Figure S8. The adsorption configurations and the Gibbs adsorption energies of H atom (ΔG_H) on the TiO_2 (101), CuO (111) and Cu_2O (111) surface.

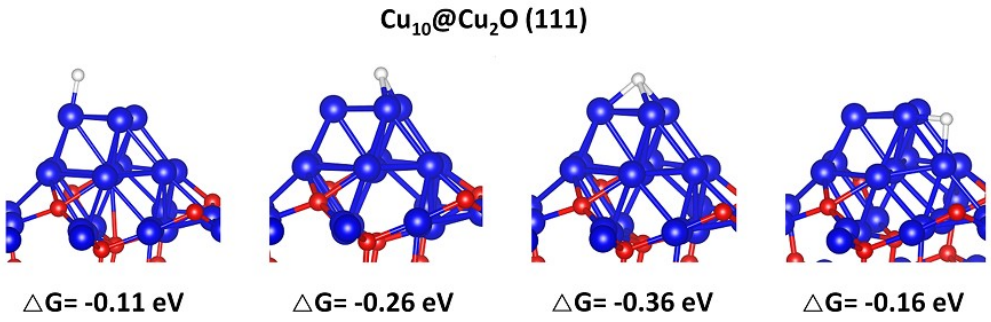

Figure S9. The adsorption configurations and the Gibbs adsorption energies of H atom (ΔG_H) at different Cu_{10} sites of the $Cu_{10}@Cu_2O$ (111) surface.

REFERENCES

(1) Li, N.; Zhang, L.; Chen, Y.; Fang, M.; Zhang, J.; Wang, H. Highly Efficient, Irreversible and Selective Ion Exchange Property of Layered Titanate Nanostructures. *Adv. Funct. Mater.* **2012,** *22*, 835-841.

(2) Kresse, G.; Hafner, J. Ab Initio Molecular Dynamics for Liquid Metals. *Phys. Rev. B* **1993,** *47*, 558-561.

(3) Kresse, G.; Furthmüller, J. Efficient Iterative Schemes for Ab Initio Total-Energy Calculations Using a Plane-Wave Basis Set. *Phys. Rev. B* **1996,** *54*, 11169-11186.

(4) Kresse, G.; Furthmüller, J. Efficiency of Ab-Initio Total Energy Calculations for Metals and Semiconductors Using a Plane-Wave Basis Set. *Comp. Mater. Sci.* **1996,** *6*, 15-50.

(5) Blöchl, P. E. Projector Augmented-Wave Method. *Phys. Rev. B* **1994,** *50*, 17953-17979.

(6) Ataei, S. S.; Mohammadizadeh, M. R.; Seriani, N. Ab Initio Simulation of the Effects of Hydrogen Concentration on Anatase TiO_2. *J. Phys. Chem. C* **2016,** *120*, 8421-8427.

(7) Huang, B. Intrinsic Deep Hole Trap Levels in Cu_2O with Self-Consistent Repulsive Coulomb Energy. *Solid State Commun* **2016,** *230*, 49-53.

(8) S. Grimme, J. Antony, S. Ehrlich and H. Krieg, A consistent and accurate ab initio parametrization of density functional dispersion correction (DFT-D) for the 94 elements H-Pu, J. Chem. Phys., **2010**, *132*, 154104

(9) Nørskov, J. K. et al. Trends in the exchange current for hydrogen evolution. *J. Electrochem. Soc.* **2005**, *152*, J23.

(10) Polliotto, V.; Livraghi, S.; Krukowska, A.; Dozzi, M. V.; Zaleska-Medynska, A.; Selli, E.; Giamello, E. Copper-Modified TiO_2 and $ZrTiO_4$: Cu Oxidation State Evolution during Photocatalytic Hydrogen Production. *ACS Appl. Mater. Interfaces* **2018,** *10*, 27745-27756.

(11) Wang, Y.; Zhou, M.; He, Y.; Zhou, Z.; Sun, Z. In Situ Loading CuO Quantum Dots on TiO_2 Nanosheets as Cocatalyst for Improved Photocatalytic Water Splitting. *J. Alloys Compd.* **2020,** *813*, 152184.

(12) Liu, Y.; Zhang, B.; Luo, L.; Chen, X.; Wang, Z.; Wu, E.; Su, D.; Huang, W. TiO_2 /Cu_2O Core/Ultrathin Shell Nanorods as Efficient and Stable Photocatalysts for Water Reduction. *Angew. Chem. Int. Ed. Engl.* **2015,** *54*, 15260-15265.

(13) Yang, K.; Cheng, G.; Chen, R.; Zhao, K.; Liang, Y.; Li, W.; Han, C. Simply Coupling TiO_2 Nanospheres with Cu_2O Particles to Boost the Photocatalytic Hydrogen Evolution through p–n Heterojunction-Induced Charge Transfer. *Energy Technol.* **2022,** 10, 2100259.

(14) Sadanandam, G.; Luo, X.; Chen, X.; Bao, Y.; Homewood, K. P.; Gao, Y. Cu Oxide Quantum Dots Loaded TiO_2 Nanosheet Photocatalyst for Highly Efficient and Robust Hydrogen Generation. *Appl. Surf. Sci.* **2021,** *541*, 148687.

(15) Hou, H.; Shang, M.; Gao, F.; Wang, L.; Liu, Q.; Zheng, J.; Yang, Z.; Yang, W. Highly Efficient Photocatalytic Hydrogen Evolution in Ternary Hybrid TiO_2/CuO/Cu Thoroughly Mesoporous Nanofibers. *ACS Appl. Mater. Interfaces* **2016,** *8,* 20128-20137.

(16) Lee, B. H.; Park, S.; Kim, M.; Sinha, A. K.; Lee, S. C.; Jung, E.; Chang, W. J.; Lee, K. S.; Kim, J. H.; Cho, S. P.; Kim, H.; Nam, K. T.; Hyeon, T. Reversible and Cooperative Photoactivation of Single-Atom Cu/TiO_2 Photocatalysts. *Nat. Mater.* **2019,** *18*, 620-626.

(17) Kum, J. M.; Yoo, S. H.; Ali, G.; Cho, S. O. Photocatalytic Hydrogen Production Over CuO and TiO_2 Nanoparticles Mixture. *Int. J. Hydrog. Energy* **2013,** *38*, 13541-13546.

(18) Moon, G. D.; Joo, J. B.; Lee, I.; Yin, Y. Decoration of Size-Tunable CuO Nanodots on TiO_2 Nanocrystals for Noble Metal-Free Photocatalytic H_2 Production. *Nanoscale* **2014,** *6*, 12002-12008.

(19) Liao, Y. T.; Huang, Y. Y.; Chen, H. M.; Komaguchi, K.; Hou, C. H.; Henzie, J.; Yamauchi, Y.; Ide, Y.; Wu, K. C. Mesoporous TiO_2 Embedded with a Uniform Distribution of CuO Exhibit Enhanced Charge Separation and Photocatalytic Efficiency. *ACS Appl. Mater. Interfaces* **2017,** *9*, 42425-42429.

(20) Wei, T.; Zhu, Y.-N.; An, X.; Liu, L.-M.; Cao, X.; Liu, H.; Qu, J. Defect Modulation of Z-Scheme TiO_2/Cu_2O Photocatalysts for Durable Water Splitting. *ACS Catal.* **2019,** *9* , 8346-8354.

(21) Chen, H.; Gu, Z.-G.; Mirza, S.; Zhang, S.-H.; Zhang, J. Hollow Cu-TiO_2/C Nanospheres Derived from a Ti Precursor Encapsulated MOF Coating for Efficient Photocatalytic Hydrogen Evolution. *J. Mater. Chem. A* **2018,** *6*, 7175-7181.